NASA DEVELOP National Program
Pop-Up Project
Summer 2022

Maipo River Valley Agriculture

Determining Crop Coefficients Using Remote Sensing for the Maipo River Valley Basin in Chile

DEVELOP Technical Report

Final – August 11th, 2022

Benjamin Goffin (Project Lead)
Duncan Srsic
Rishudh Thakur
Sarah Da Conceicao Carlos

Advisors:
Dr. Kenton Ross, NASA Langley Research Center (Science Advisor)
Dr. Venkataraman Lakshmi, University of Virginia (Science Advisor)

Fellow:
Caroline Williams (PUP Fellow)

1. Abstract

Agriculture is the primary use of water in the Maipo River basin of Central Chile, accounting for ~ 75% of the total demand. Assessment of irrigation needs for agricultural production has commonly relied on reference crop coefficients (Kc) derived from geographic and climatic conditions that differ from those of Chile. In partnership with the Centro de Información de Recursos Naturales (CIREN), this work focused on calculating site-specific crop coefficients tailored to crop production in the water-stressed Maipo River Valley. Two distinct approaches were implemented, each relying on remotely-sensed Earth observation datasets from NASA over consecutive growing seasons from 2019 to 2022. The first method estimated Kc values based on their linear relationship with the Normalized Difference Vegetation Index (NDVI) obtained from either Terra Moderate Resolution Imaging Spectroradiometer (MODIS) or Landsat 8 Operational Land Imager (OLI) surface reflectance. The second technique leveraged information from the ISS Ecosystem Spaceborne Thermal Radiometer Experiment on Space Station (ECOSTRESS) by computing the ratio between actual crop evapotranspiration (ET) and potential evapotranspiration (PET). Both procedures showed promising results that can build on one another. The former approach best captured vegetation signals of annual crops while the latter appeared suited for perennials. Overall, this study provides a strong basis and novel way to accurately estimate Kc using remote sensing, with the potential for improved irrigation management and reduction in water consumption.

Key Terms
Crop Coefficient, Evapotranspiration, Irrigation Needs, Water Scarcity, LANDSAT, MODIS, ECOSTRESS

2. Introduction

2.1 Background Information

The Maipo River in Central Chile flows from the Andes Mountain to the Pacific Ocean, collecting water over approximately 15,300 km^2 that encompass the Santiago metropolitan area (Figure 1). The Maipo River Basin provides livelihood to nearly 40% of the Chilean population and contributes to roughly 44% of Chile's Gross Domestic Product (Bauer, 2017). With its Mediterranean climate, the region is an agricultural hub producing a range of crops (Figure A1). However, annual precipitations are concentrated in the winter months, causing the agricultural sector to rely on irrigation and use roughly three-quarters of the basin's water (Peña-Guerrero et al., 2020; World Bank, 2011). Most of these irrigated areas depend on water withdrawals from surface flows (Rosegrant et al., 2000). But water availability is becoming a concern as this semi-arid region is experiencing increasingly dryer conditions with a decrease in precipitation and increase in temperatures (Falvey et al., 2009; Dai, 2011; Boisier et al., 2016). Climate-related changes are affecting runoff and streamflow, posing the threat of water supply shortages (Magrin et al., 2014). Additionally, Chile has been affected by a multi-year drought beginning in 2010 and extending to present (August 2022) that exacerbated the water deficit (Rangecroft et al., 2016). Based on an assessment by World Resources Institute (WRI), extremely high levels of baseline water stress have been observed across the Maipo River Basin with water withdrawals exceeding 80% of the available supply from surface and groundwater annually (Hofste et al., 2019). The potential aridification of the Maipo region and the

ongoing drought could further alter the water availability for cities, hydropower generation, and agriculture. More competition across sectors for water withdrawal in the Maipo River Valley puts irrigated agriculture at risk and calls for research on irrigation practices tailored to the region's crop-specific water requirement.

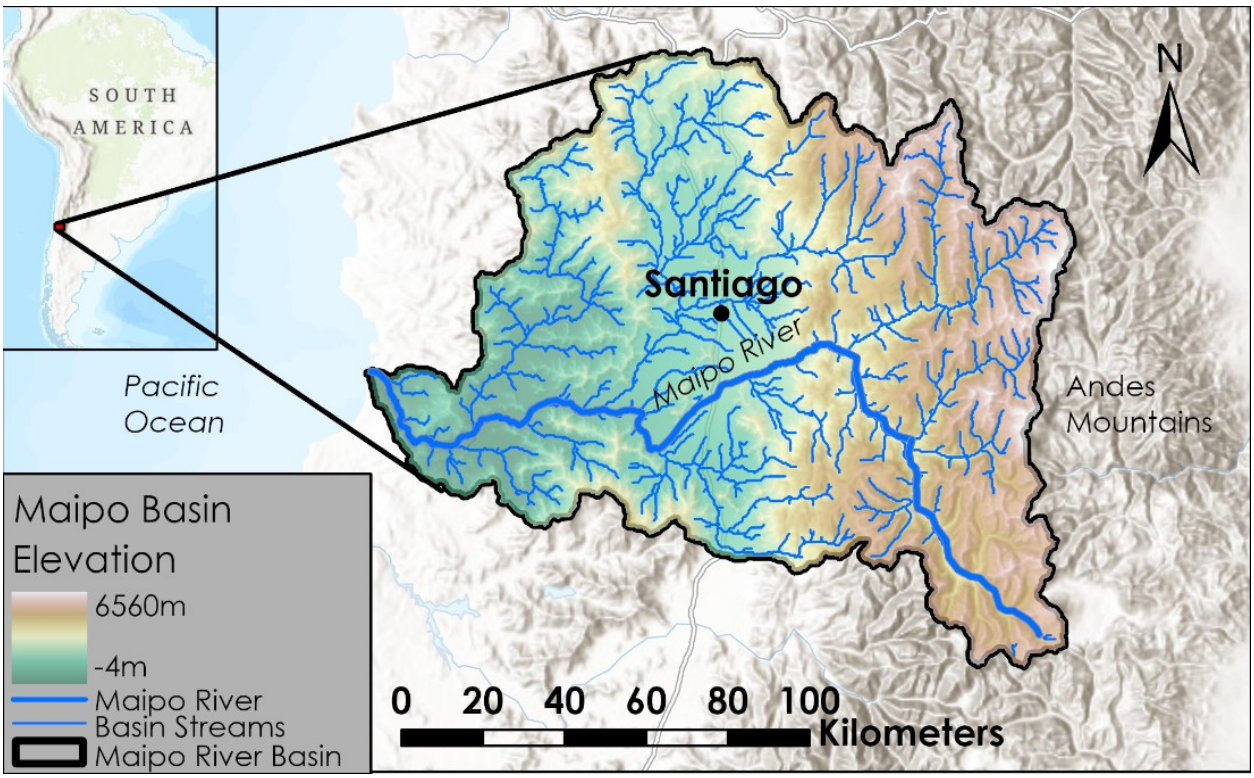

Figure 1. Elevation map of the Maipo River basin and streams.
[Base map credits: Esri, FAO, NOAA, USGS, CGIAR, HERE, Garmin, NASA, WWF, IDE Chile]

Crop water requirements and irrigation needs are based on crop evapotranspiration (ETc). ETc is often calculated as the product of two factors: the reference or potential evapotranspiration (ETo or PET) based on climatic parameters and a crop coefficient (Kc) value that accounts for site constraints and converts ETo to ETc for a given crop. However, Kc (and therefore ETc estimates) can vary significantly in different parts of the world and under varying climates (Guerra et al., 2016). Crop coefficients also fluctuate as plants reach different growth stages. The same can be said about crop greenness and vegetation reflectance throughout the growing season. Previous work has drawn relationships with good correlation between Kc and remotely sensed vegetation indices such as the Normalized Difference Vegetation Index, also known as NDVI (Singh & Irmak, 2009; Kamble et al., 2013). While Kc modeling has proved successful using Earth observations (EO), others have gone as far as to demonstrate that farmers could reduce their irrigation volumes by nearly one-fifth using updated ETc estimates from satellite remote sensing techniques (Reyes-González et al., 2018).

Frequently used Kc values from Allen et al. (1998) were based on areas with differing geographic and climate conditions than those of Chile, resulting in potentially inaccurate assessments of water requirements specific to the Maipo

River basin (Figure A2). Previous scientific studies give ground for a remotely sensed determination of site-specific Kc values that will inform irrigation practices in the water-stressed Maipo River Valley. For this feasibility project, the team selected study sites within the Maipo River Basin to capture consistency and variability in geographic and climatic conditions across the region. Annual and perennial crops of interest to the partners were maize (*Zea mays*) and English walnut (*Juglans regia*), respectively. EO were analyzed during the crops' growth stages (September to May) of consecutive growing cycles from 2019 to 2022.

2.2 Project Partners & Objectives

On the ground and through the use of geospatial technologies, the Centro de Información de Recursos Naturales (CIREN) works to advance land-use planning, resource management, and public decision-making in Chile. In 2021, CIREN performed a study examining the demand for water of agricultural production among four watersheds including the Maipo River basin. In that process, concerns were raised about relying on standardized crop coefficients from FAO guidelines and a need was identified for linear models and Kc values that would capture the geographic and climate conditions of Chile.

Our DEVELOP team collaborated with CIREN and the Embassy of Chile, Agricultural Office to enhance current approaches for assessing irrigation needs. Specifically, we leveraged NASA EO datasets to obtain crop coefficients specific to the geographic and climatic conditions of the Maipo River Valley. Furthermore, we compared different Kc methodologies and confirmed Kc estimates between crop types through growing seasons and across the region. Last, we assessed actual evapotranspiration and water demand of agricultural production based on remotely sensed information.

3. Methodology

3.1 Data Acquisition

The team acquired data for the time period from September to May, between 2019 and 2022 for the study area. Primary EOs used include Landsat 8OLI, Terra MODIS, and the ISS ECOSTRESS (Table 1). For NDVI calculations, we utilized level 2 surface reflectance data from Landsat 8 OLI (Masek et al., 2006; Vermote et al., 2016). In addition, we obtained ET and PET products from ISS ECOSTRESS (Hook & Fisher, 2019). We also relied on PET information from Terra MODIS (Didan, 2021; Running et al., 2021).

Table 1
Acquired Data and Data Sources

Platform & Sensor	Data Source	Parameter	Time Period
Landsat 8 OLI	Google Earth Engine	Surface Reflectance	2019–2022 (September–May)
Terra MODIS	Google Earth Engine	ET	2019–2022 (September–May)
ISS ECOSTRESS	NASA AppEEARS	ET & PET	2019–2022 (September–May)

In addition, several ancillary datasets were instrumental in the site selection (detailed in Section 3.3). The watershed limits were based on basin delineation from the Infraestructura de Datos Geoespaciales de Chile (IDE Chile) límite de la cuenca del Río Maipo. Partner organization CIREN provided two additional datasets, with a geospatial database of agricultural parcels (i.e. ‘uso de suelo actual cuenca del Río Maipo’) and a phenological calendar for the region (i.e. ‘calendario de fenología de cultivos dentro de la cuenca del Río Maipo’). While the

former informed on the type and extent of the agricultural production, the latter consisted of the timeframes for sowing, flowering, harvesting and leaf fall of crops such as Maize and English walnut as summarized in Table 2. Typical crop coefficient values and development stage durations were taken from the FAO irrigation and drainage paper No. 56 (Allen et al, 1998). Digital land elevation data for the Maipo River basin came from NASA's Shuttle Radar Topography Mission (SRTM).

Table 2
Approximate Timeframe of Growth Stages for Crop Types (from CIREN)

Growth Stages/ Crop Types	Sowing	Flowering	Defoliation	Harvest
Maize	Sep 8 to Oct 14	Nov 1 to Dec 14	*N/A*	Dec 22 to Mar 28
English Walnut	*N/A*	Sep 8 to Oct 7	Apr 8 to May 7	May 8 to Jun 7

3.2 Data Processing

We composited the ET and PET product from ECOSTRESS using Esri ArcGIS Pro 3.0.0 for each growing season. Thereafter, our team uploaded all EOs to Google Earth Engine (GEE) and performed additional processing using the JavaScript Application Programming Interface (API). The data were clipped to the basin extents on the GEE platform. Using the pixel Quality Assessment (QA) bands on GEE, we considered the impact of cloud cover on Landsat reflectance and masked pixels containing cloud cover or cloud shadow. We then used the resulting raster of red and near-infrared (NIR) bands was to calculate NDVI using the Equation 1 below (Tucker, 1979):

$$NDVI = \frac{NIR - RED}{NIR + RED} \quad (1)$$

3.3 Data Analysis

Our team selected 16 study sites for data analysis: 4 English walnut orchards (labeled WA) and 12 maize fields (labeled CO). To capture redundance and variability in geographic and climate conditions, sites for each crop included locations in a lower elevation range between 100 and 200 m above mean sea level (labeled LO) along with some at higher elevations around 400 meters (labeled HI). These locations are spread over a large spatial distribution from Melipila and Maria Pinto to the West, to the vicinity of Santiago and Laguno de Acuelo to the East (Figure B1). Our partners indicated that the former two had particularly large agricultural activities while the latter two experienced increasing water stress. Next, we subtracted a buffer of 50 m into the site parcels to reduce contamination from nearby pixels and potential edge effects along an agricultural field (Figure B2). We considered buffered parcels ranging in size, with a minimum acreage of 3 ha or at least 30 NDVI pixels as indicated in Table 3 below. We then utilized Python 3.7.13 on Google Colab to convert the processed raster data into data frames at each site. Further analyses were performed separately for the two methodologies detailed below.

Table 3
Geographic Variables and Parcel Characteristics of Study Sites

Elevation Range (m)	Nearby Locality	Crop Type	Site Designation	Parcel Size (ha)
100–200	Melipilla	Maize	CO-LO-101 CO-LO-102 CO-LO-103	77 62 103
100–200	Melipilla	English Walnut	WA-LO-101 WA-LO-102	28 17
100–200	Maria Pinto	Maize	CO-LO-104 CO-LO-105 CO-LO-106	13 27 12
300–400	Talagante	Maize	CO-HI-101 CO-HI-102 CO-HI-103	4 4 3
300–400	Laguna de Aculeo	Maize	CO-HI-104 CO-HI-105 CO-HI-106	7 8 6
400–500	Lampa	English Walnut	WA-HI-101 WA-HI-102	125 23

3.3.1 NDVI – based Kc Methodology

The NDVI-based crop coefficient approach relied on the FAO-Kc curve and leveraged added information found in NDVI signals. This method built on the relationship and variability in between these datasets to produce site-specific Kc as shown in Figure 2. To study the linkage between the datapoints of NDVI and corresponding Kc, our team aggregated spatial arrays of NDVI values across each site into an average for each day of record. For reference Kc, we used typical values and stages from Allen et al.(1998). We interpolated those reference Kc values for the particular dates of NDVI observations.

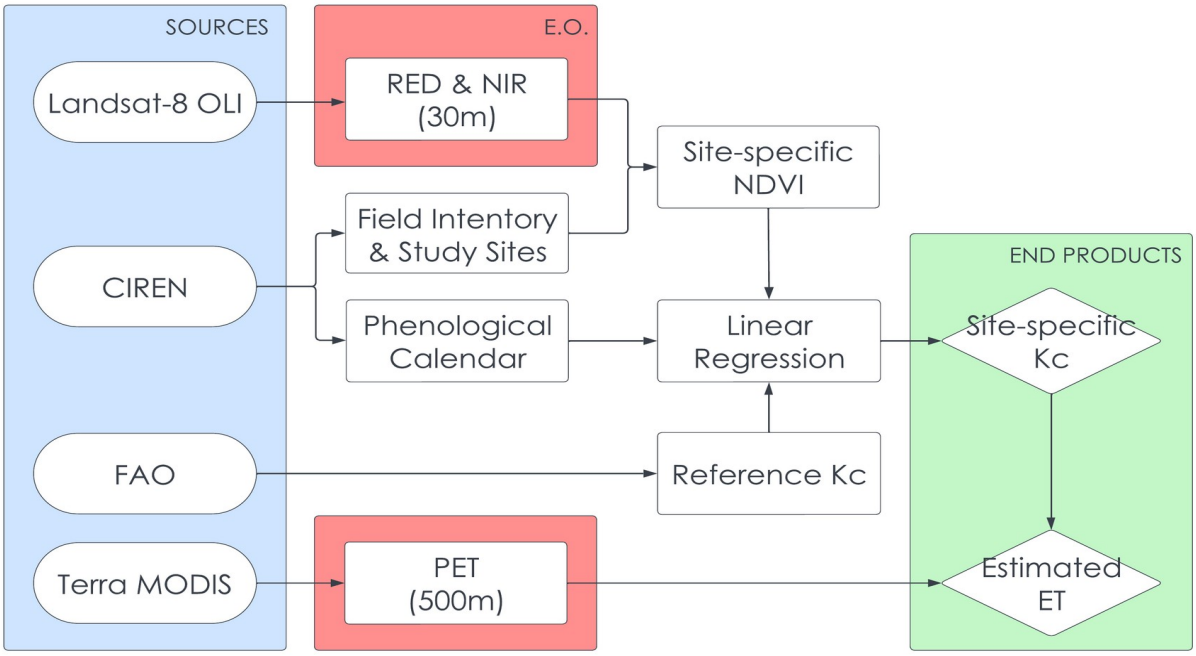

Figure 2. NDVI-based Kc methodology

Thereafter, we aimed to match the seasonal pattern in NDVI with the reference Kc curve at each of the 12 maize sites. Through the iterative process illustrated in Figure 3, we adjusted how far along the growing cycle a crop was likely to be when the observations of NDVI were made. Accounting for the most likely day of planting in the growing cycles of each site enabled us to consider days after planting instead of dates in the year, thus filtering out some of the temporal variability in agricultural practices across sites.

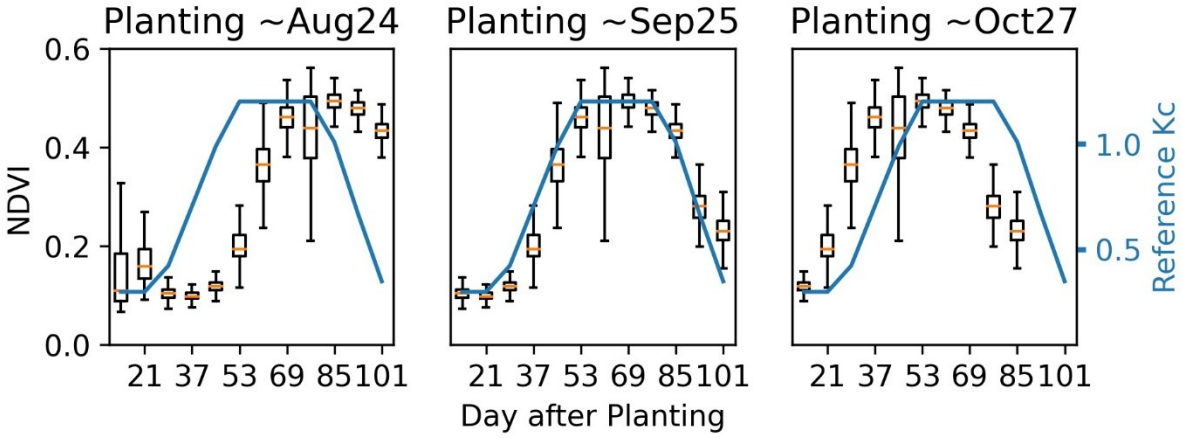

Figure 3. Iterations of the assumed day of planting for NDVI values at site CO-LO-101 in growing cycle 2021–2022. Based on reference Kc curve from FAO, the middle frame appeared to be the most likely scenario.

We proceeded by dividing the 12 maize sites into two categories: those for model fitting and those for validation purposes. We performed linear regressions at 8 of the 12 sites, as indicated in Table 4 below. For each of these sites, we derived model parameters of Kc as a function of NDVI across 3 years of data.

Table 4.
Use of Maize Sites in Model Fitting

Site Designation	Used for
CO-HI-101	Linear Regression
CO-HI-102	Ensemble Validation
CO-HI-103	Linear Regression
CO-HI-104	Linear Regression
CO-HI-105	Ensemble Validation
CO-HI-106	Linear Regression
CO-LO-101	Linear Regression
CO-LO-102	Ensemble Validation
CO-LO-103	Linear Regression
CO-LO-104	Linear Regression
CO-LO-105	Ensemble Validation
CO-LO-106	Linear Regression

To produce a single model applicable to the whole basin, an ensemble equation was developed by taking the mean of each regression parameter across all 8 sites. The mean ensemble equation was compared with those obtained by taking the median and averaging with weighted R-squared. Being relatively consistent, the project was further advanced with the mean ensemble approach.

We then applied our model at the 4 sites that had been set aside for this validation step. New crop coefficients were estimated using the NDVI observations of the sites across the study period. To assess the robustness of the model, we compared the site-specific Kc values against the Kc reference. We also studied the performance of the regional ensemble with respect to individual models derived from the best-fit regression at each validation site. We considered the difference in between these estimates and assessed the any potential bias in our model.

Finally, our team demonstrated the application of the NDVI–Kc model (derived and validated) over the course of a growing cycle at two of the validation sites. Along with site-specific Kc estimates based on NDVI, we acquired potential evapotranspiration data from Terra MODIS and interpolated it for the days at which we had modeled Kc. Last, we multiplied PET by modeled Kc to estimate actual evapotranspiration.

3.3.2 ETc – based Kc Methodology

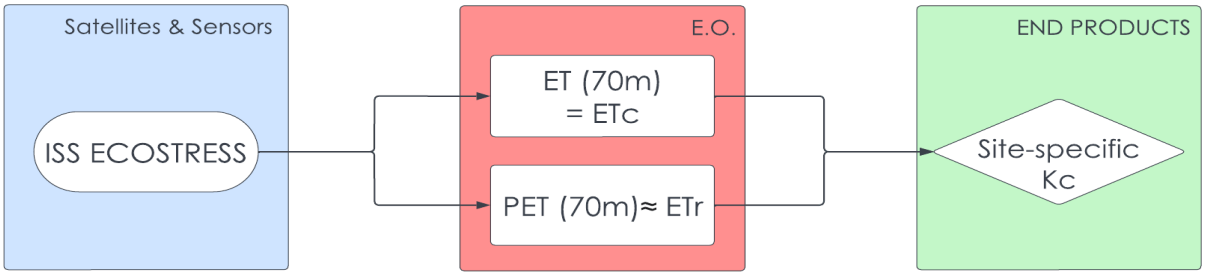

Figure 4. ETc-based Kc methodology

The ETc-based crop coefficient approach is based on the actual crop evapotranspiration (ETc) and reference evapotranspiration (ETo) products from the ISS ECOSTRESS mission at 70 m resolution (Figure 4). Our team reviewed the variability in the two dataset and applied a moving average across each timeseries to filter out some of the noise. Thereafter, we calculated the ratio of the two variables at one site to obtain Kc over time as shown in the Equation 2 below (Allen et al, 1998).

$$K_c = \frac{ET_c}{ET_r} \qquad (2)$$

In addition, we merged the Kc estimates over the first 100 days of the growing cycle to capture the significant water requirement during the development stage of the English walnut. Once calculated, the typical crop coefficient obtained for a growth stage at a site does not require a model input like the prior approach. As such, a site-specific Kc value can readily convert PET into ET.

4. Results & Discussion

4.1 Analysis of Results

4.1.1 NDVI – based Kc Methodology

In reviewing the spatial distribution of NDVI over time, our team observed a range of signals over the growing cycle of maize (Figure C1). Based on information from the Table 2, we recognized successive growth stages in the remotely sensed vegetation response. We found that NDVI values increased following seeding, reached a plateau in the mid-season, and decreased as the plant experienced senescence. Our team was able to align this typical pattern in NDVI with the reference Kc curve to identify the most likely date of planting. Working within the growth cycle timeframes provided by our partner, we were able to establish when seeding occurred in 31 of the 36 combinations for the 12 sites and 3 seasons we studied (Table 5). Assumed day of planting ranged from the beginning of September to the end of October.

Table 5.
Assumed Day of Planting for Maize Sites and Seasons

Site Designation	2019-2020	2020-2021	2021-2022
CO-HI-101	Oct-22	*N/A*	Oct-27
CO-HI-102	Sep-04	Oct-08	Sep-25
CO-HI-103	Sep-04	*N/A*	Sep-09
CO-HI-104	Sep-04	Sep-06	*N/A*

CO-HI-105	Sep-20	Sep-22	Sep-09
CO-HI-106	Sep-04	Sep-22	Sep-09
CO-LO-101	Sep-04	Sep-06	Sep-25
CO-LO-102	Sep-20	Sep-06	Sep-25
CO-LO-103	Sep-20	Sep-06	*N/A*
CO-LO-104	Oct-22	Oct-08	Oct-11
CO-LO-105	Oct-22	Oct-08	Oct-11
CO-LO-106	Sep-04	Sep-06	*N/A*

When plotting Kc against corresponding NDVI at 8 sites, we observed a generally linear trend between the two datasets (Figure C2). Our team found R-squared scores around 0.61 to 0.89, implying that most variations in Kc can be explained linearly by NDVI. We hypothesized that NDVI was also capturing site-specific responses, not taken into account by the theoretical FAO curve. From our linear regressions, we obtained 8 sets of slope parameter and intercept (or constant) as shown in Table 6 below. The fields in the low elevation range had lower slope coefficients (in the range of 2.12 to 2.58) compared to the higher elevation parcels (with slopes of 2.58 to 3.01). This meant that a relatively greater coefficient was needed to match FAO Kc in higher sites where NDVI signals were potentially not as strong. We also noted that the two lower coefficients of determination were found near Maria Pinto. Our team suspected that water stress and/or irrigation practices in the area might have impacted vegetation signals.

Table 6.
Linear Regression Parameters and Ensemble Formulation for Maize Sites

Site Designation	Regression Slope	Regression Intercept	Regression R-squared
CO-LO-101	2.451	0.024	0.878
CO-LO-103	2.582	-0.003	0.859
CO-LO-104	2.125	0.184	0.738
CO-LO-106	2.344	0.236	0.614
CO-HI-101	3.014	0.176	0.838
CO-HI-103	2.581	0.174	0.854
CO-HI-104	2.669	0.123	0.891
CO-HI-106	2.794	0.098	0.855
Averaged-Ensemble Eq.	*2.57*	*0.13*	N/A

During validation of the ensemble model, NDVI-Kc estimates appeared to follow the FAO-Kc curve closely over the growing seasons at 4 sites (Figure C3). When plotting one variable against the other, we observed that the datapoints fell generally near the 1:1 line (Figure 5). This signified that the modeled Kc remained strongly correlated to the reference values. Per the R-squared scores ranging from 0.56 to 0.90 (Figure 5), we found that NDVI-Kc was not entirely dependent on the FAO-Kc. However, the amount of residual was low with RMSE between 0.01 and 0.06 (on the order of 2 to 7%), therefore, our team determined the quality of the prediction to be high.

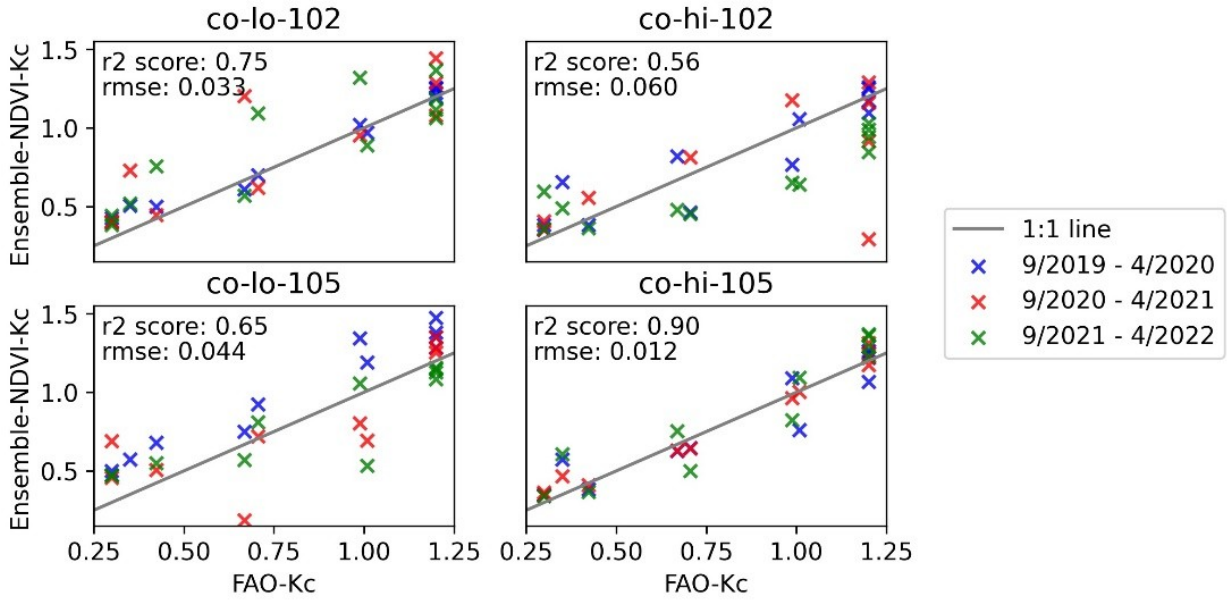

Figure 5. NDVI-Kc ensemble validation against FAO reference at 4 maize sites over 3 growing seasons

Additionally, we compared the modeled values from the ensemble to those of individual best-fit specific to each validation site and found similar outputs (Figure C4). As anticipated, the site-specific regressions explained more variations in NDVI

with respect to FAO-Kc at each site and yielded greater R-squared scores. However, the benefit of a site-specific regression appeared to be marginal, implying that the regional model captured most of the vegetation signals across validation sites.

When looking into the potential bias of the model and investigating the difference in Kc estimates from the ensemble equation and best-fit at each site, we observed a slight overestimation at the sites in the lower elevation range along with an underestimation at one of the two higher elevation sites (Figure C5). Overall, the residuals appeared to balance out with no particular pattern observed. Based on these results, no further tuning of our ensemble parameters was deemed necessary, and our team concluded that the model could be used to determine crop coefficients for maize fields across the Maipo River basin.

Using NDVI inputs, our Kc model, and PET observations, we produced a novel set of ET estimates for the growing season of two sites. In the first case (Figure 6), we found that our values plotted below those of the FAO, implying a potential overestimation of irrigation needs per the FAO reference alone. For the second case, we obtained more nuanced findings, with both a potential prior underestimation by FAO in the first half of the season along with a possible overestimation of water requirements in the second half of the season (Figure C6).

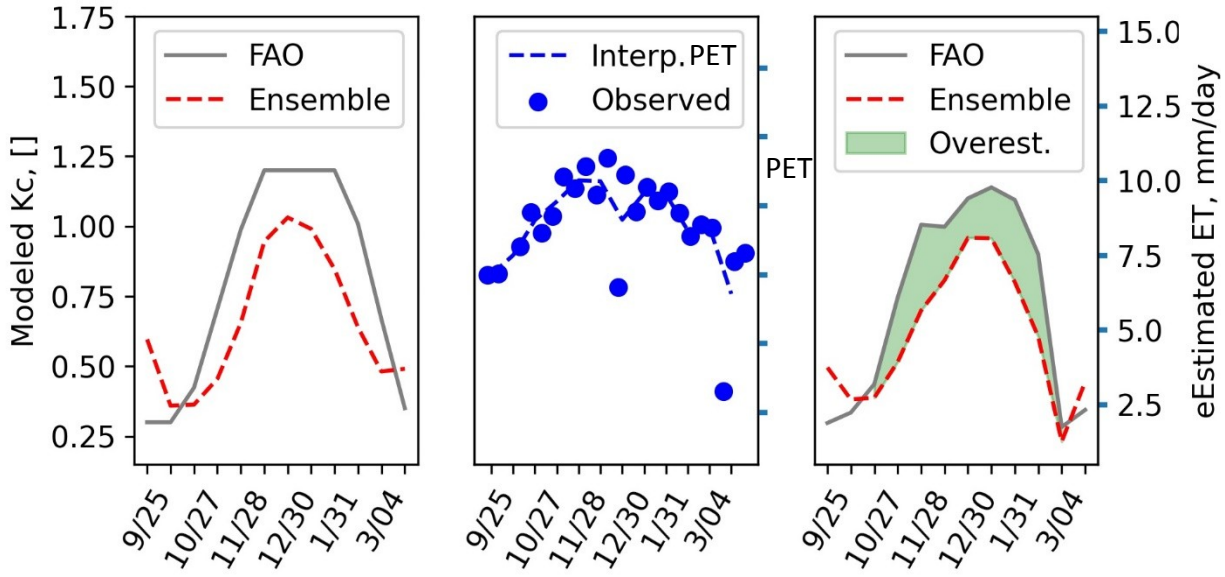

Figure 6. Applications of ensemble Kc model (left) along with PET (middle) for water requirement estimation (right) at site CO-HI-102 in growing season 2021–2022

4.1.2 ETc – based Kc Methodology

After failing to sense meaningful variations over the successive growth stages of the English walnut by looking at NDVI (Figures C7 & C8), our team explored a second methodology. Our team studied ET and PET products from ECOSTRESS and observed that the observed values varied widely. We hypothesized that observations were influenced by various terrestrial changes in undergrowth,

irrigation patterns, or weather conditions along with the sensor having no fixed revisit period over the season or time of day. Because of this, no clear indication of flowering and harvest of the English walnut could be inferred from snapshots in time of ET (Figure C9).

Only after applying a moving average to both ET and PET were we able to successfully filter out some noise at this particular site and given season (Figure C10). We identified an averaged Kc of 0.80 in the first 100 days of the growing cycles, as denoted by the dash line in Figure 7. This value is thought to be representative of the development stage of the English walnut, with the potential to capture the significant water requirement during that timeframe.

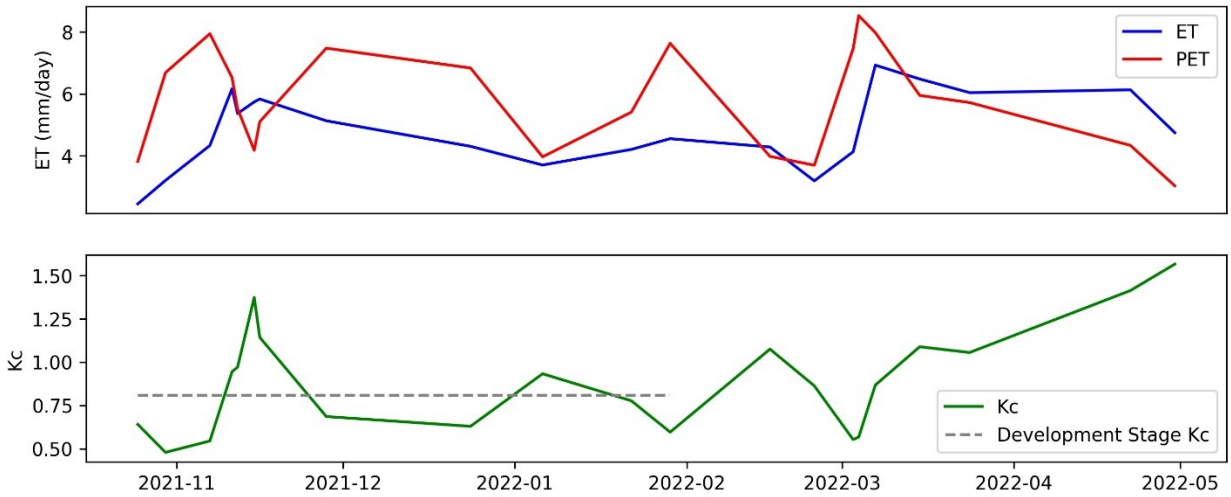

Figure 7. Variability in evapotranspiration and Kc estimates at site WA-LO-101 in growing season 2021–2022.

4.2 Future Work

Further statistical analyses across elevation ranges could add insightful information to the first methodology. Along those lines, our partner recommended that a range of applicability for input values of NDVI be added to our model. This work could also be expanded to account for additional years and more sites. This is of particular interest with ECOSTRESS as only one growing cycle for a given site was considered and limited sampling with significant noise was encountered. To strengthen the robustness of our techniques, more comparisons could be drawn between datasets of NDVI and PET across MODIS and ECOSTRESS. In addition, in-situ data from flux towers and pan evaporation could corroborate some of the PET and ET estimates. Lastly, this approach could be applied to other crop types, particularly tomato fields which were suggested by our partner s as a next step.

5. Conclusions

Chile has recently ranked 18th of the most water-stressed country in the world (Hofste et al., 2019). The FAO has also predicted that conditions could worsen with desertification and salinization potentially affecting 50% of agricultural lands in all Latin America by 2050 (FAO, 2004). Our team collaborated with CIREN and the Embassy of Chile, Agricultural Office to improve irrigation need assessment and generate site-specific crop coefficients tailored to the agricultural production of

the Maipo River Valley in Central Chile. This project leveraged NASA Earth observations and identified two approaches based on remote sensing from space. A NDVI-based and ETc-based Kc techniques were implemented, validated, and compared between crop types, through growing seasons, and across the region. Specifically, we produced a NDVI-based Kc model for maize that incorporates vegetation health to assess crop water requirements. We also calculated typical Kc values during the development stage of the English walnut based on EOs.

Study findings provided partner organizations with tested methodologies to follow for Kc calculation, application, and limitation. Findings will assist CIREN in evaluating water demands and improving irrigation management approach in Chile's agricultural regions. To further alleviate water scarcity and provide greater community resilience, these end products will also be shared with other organizations such as the Comisión Nacional de Riego (CNR) and the Fundación Para la Innovación Agraria (FIA) to support their decision making around agriculture and irrigation.

6. Acknowledgments

The Maipo River Valley team would like to thank our partners from the Centro de Información de Recursos Naturales (CIREN) and the Embassy of Chile, Agricultural Office for their collaboration and insight on this project. The team would also like to thank our science advisors Dr. Kenton Ross and Dr. Venkataraman Lakshmi, and our DEVELOP fellow Caroline Williams for their guidance and support throughout the project’s duration. Finally, we thank DEVELOP’s Project coordination Fellows Tamara Barbakova and Robert Cecil Byles for their suggestions and editing.

Maps throughout this work were created using ArcGIS® software by Esri. ArcGIS® and ArcMap™ are the intellectual property of Esri and are used herein under license. All rights reserved.

Any opinions, findings, and conclusions or recommendations expressed in this material are those of the author(s) and do not necessarily reflect the views of the National Aeronautics and Space Administration.

This material is based upon work supported by NASA through contract NNL16AA05C.

7. Glossary

Aridification – The gradual change of a region from a wetter to a drier climate.
Centro de Información de Recursos Naturales (CIREN) – CIREN works to ensure decision-making on irrigation management, and land use policies in Chile. In this project, CIREN contributed greatly with local knowledge and in-situ data.
Crop Evapotranspiration (ETc) – The amount of water transpired by plants to the atmosphere.
Desertification – A type of land degradation in drylands in which biological productivity is lost due to natural processes or induced by human activities whereby fertile areas become increasingly arid.
ECOSTRESS – ECOsystem Spaceborne Thermal Radiometer Experiment on Space Station.
Earth observations (EO) – Satellites and sensors that collect information about the Earth's physical, chemical, and biological systems over space and time.
Evapotranspiration (ET) – The process by which water is transferred by the soil surface and transpiration by plants from the land to the atmosphere.
Food and Agriculture Organization (FAO) – Food and Agriculture Organization of the United Nations that specializes in the fight against world hunger.
Intergovernmental Panel on Climate Change (IPCC) – A United Nation organization that is responsible for advancing knowledge on human-induced climate change.
LANDSAT 8 Operational Land Imager (OLI) – A satellite and sensor that rotates around the Earth every 16 days and measures in the visible, near infrared, and shortwave infrared portions (VNIR, NIR, and SWIR) of the spectrum.
MODIS – Moderate Resolution Imaging Spectroradiometer is a sensor aboard Terra satellite that collects various data by viewing the entire Earth's surface every 1 to 2 days.
Normalized Difference Vegetation Index (NDVI) – A simple graphical indicator that can be used to analyze remote sensing measurements, often from a space platform, assessing whether or not the target being observed contains live green vegetation.
Potential Evapotranspiration (PET) – The amount of evaporation that would occur if a sufficient water source were available.
Quality Assessment (QA) – The data collection and analysis through which the degree of conformity to predetermined standards and criteria are exemplified.
Reference Evapotranspiration (ETo) – The estimation of evapotranspiration of a reference field that assumes the field is large of four to seven-inch tall, cool season grass that has unlimited water availability.
Remote sensing – The acquisition of information from a distance via remote sensors on satellites and aircraft that detect and record reflected or emitted energy.
R-squared (or Coefficient of Determination) – A statistical measure that represents the proportion of the variance for a dependent variable that's explained by an independent variable or variables in a regression model.
Root Mean Square Error (RMSE) – Used measure of the differences between values predicted by a model or an estimator and the values observed.
Senescence – The process of aging in plants.
Water Scarcity – The limited water availability due to climate change, change in water balance, and other factors.

World Resources Institute (WRI) – A research organization that aims to develop practical solutions that improve people's lives and ensure nature can thrive.

8. References

Allen, R. G., Pereira, L. S., Raes, D., & Smith, M. (1998). *Crop evapotranspiration-Guidelines for computing crop water requirements-FAO Irrigation and drainage paper 56.* Food and Agriculture Organization (FAO) of the United Nations, Rome. https://www.fao.org/3/x0490e/x0490e00.htm

Bauer, C. J. (2017). *The evolving water market in Chile's Maipo River Basin: A case study for the political economy of water markets project.* Ecosystem Economics LLC, AMP Insights LLC, and the Rockefeller Foundation. https://static1.squarespace.com/static/56d1e36d59827e6585c0b336/t/5805460515d5dbb1ab599b91/1476740618944/Chile-Maipo-Bauer.pdf

Boisier, J. P., Rondanelli, R., Garreaud, R.D., & Muñoz, F. (2016). Anthropogenic and natural contributions to the Southeast Pacific precipitation decline and recent megadrought in central Chile. *Geophysical Research Letters*, *43*(1), 413–421. https://doi.org/10.1002/2015GL067265

Dai, A. (2012). Erratum: Drought under global warming: A review. *Wiley Interdisciplinary Reviews: Climate Change*, *3*(6), 617–617. https://doi.org/10.1002/wcc.81

Didan, K. (2021). *MODIS/Terra Vegetation Indices 16-Day L3 Global 250m SIN Grid* V06*1* [Data set]. NASA EOSDIS Land Processes DAAC. Retrieved July 5, 2022, from https://doi.org/10.5067/MODIS/MOD13Q1.061

Tucker, C. J. (1979). Red and photographic infrared linear combinations for monitoring vegetation. *Remote Sensing of Environmen*t, *8*(2), 127–150. https://doi.org/10.1016/0034-4257(79)90013-0.

Falvey, M., & Garreaud, R.D. (2009). Regional cooling in a warming world: Recent temperature trends in the southeast Pacific and along the west coast of subtropical South America (1979 – 2006), *Journal of Geophysical Research: Atmospheres*,*114*(D4) D04102. https://doi.org/10.1029/2008JD010519

FAO (2004). *28ava Conferencia Regional de la FAO para América Latina y el Caribe*. Food and Agriculture Organization (FAO) of the United Nations, Ciudad de Guatemala, Guatemala. https://www.fao.org/3/J1697s/J1697s.htm

Guerra, E., Ventura, F., & Snyder., R.L. (2016). Crop coefficients: A literature review. *Journal of Irrigation and Drainage Engineering*, *142*(3). https://doi.org/10.1061/(ASCE)IR.1943-4774.0000983

Hofste, R. W., Kuzma, S., Walker, S., Sutanudjaja, E. H., Bierkens, M. F., Kuijper, M. J., Sanchez, M. F., Van Beek, R., Wada, Y., Rodríguez S. G., & Reig, P. (2019). *Aqueduct 3.0: Updated Decision Relevant Global Water Risk Indicators.* World Resources Institute. https://doi.org/10.46830/writn.18.00146

Hook, S., Fisher, J. (2019). *ECOSTRESS Evapotranspiration PT-JPL Daily L3 Global 70 m* V001 [Data set]. NASA EOSDIS Land Processes DAAC. Retrieved July 5, 2022, from https://doi.org/10.5067/ECOSTRESS/ECO3ETPTJPL.001

Kamble, B., Kilic, A., & Hubbard, K. (2013). Estimating Crop Coefficients Using Remote Sensing-Based Vegetation Index. *Remote Sensing*, *5*(4), 1588–1602. https://doi.org/10.3390/rs5041588

Magrin, G.O., Marengo, J.A., Boulanger, J.-P., Buckeridge, M.S., Castellanos, E., Poveda, G., Scarano, F.R. & Vicuña, S. (2014). Central and South America. *Climate Change 2014: Impacts, Adaptation, and Vulnerability. Part B: Regional Aspects.* Contribution of Working Group II to the Fifth Assessment Report of the Intergovernmental Panel on Climate Change, Barros, V.R., Field, C.B. Dokken, D.J., Mastrandrea, M.D., Mach, K.J., Bilir, T.E., Chatterjee, M., Ebi, K.L., Estrada, Y.O., Genova, R.C., Girma, B., Kissel, E.S., Levy, A.N., MacCracken, S., Mastrandrea, P.R., and White, L.L., Eds., Cambridge University Press, Cambridge, United Kingdom and New York, NY, USA, pp. 1499–1566. https://www.ipcc.ch/site/assets/uploads/2018/02/WGIIAR5-PartB_FINAL.pdf

Masek, J.G., Vermote, E.F., Saleous N.E., Wolfe, R., Hall, F.G., Huemmrich, K.F., Gao, F., Kutler, J., and Lim, T-K. (2006). A Landsat surface reflectance dataset for North America, 1990–2000. *IEEE Geoscience and Remote Sensing Letters*, *3*(1), 68–72. http://dx.doi.org/10.1109/LGRS.2005.857030

Peña-Guerrero, M. D., Nauditt, A., Muñoz-Robles, C., Ribbe, L., & Meza, F. (2020). Drought impacts on water quality and potential implications for agricultural production in the Maipo River Basin, Central Chile. *Hydrological Sciences Journal, 65*(6), 1005–1021. https://doi.org/10.1080/02626667.2020.1711911

Rangecroft, S., Van Loon, A.F., Maureira, H., Verbist, K., & Hannah, D.M. (2016). Multi-method assessment of reservoir effects on hydrological droughts in an arid region. *Earth System Dynamics*, [preprint] , https://doi.org/10.5194/esd-2016-57

Reyes-González, A., Kjaersgaard, J., Trooien, T., Hay, C., & Ahiablame, L. (2018). Estimation of crop evapotranspiration using satellite remote sensing-based vegetation index. *Advances in Meteorology*, *2018*. https://doi.org/10.1155/2018/4525021

Rosegrant, M.W., Ringler, C., McKinney, D.C., Cai, X., Keller, A., & Donoso, G. (2000). Integrated economic-hydrologic water modeling at the basin scale: The Maipo river basin. *Agricultural Economics*, *24*(1), 33–46. https://doi.org/10.1111/j.1574-0862.2000.tb00091.x

Running, S., Mu, Q., Zhao, M. (2021). *MODIS/Terra Net Evapotranspiration 8-Day L4 Global 500m SIN Grid* V061 [Data set]. NASA EOSDIS Land Processes DAAC. Retrieved July 5, 2022, from https://doi.org/10.5067/MODIS/MOD16A2.061

Singh, R., & Irmak, A. (2009). Estimation of Crop Coefficients Using Satellite Remote Sensing. *Journal of Irrigation and Drainage Engineering, 135*(5). https://doi.org/10.1061/(ASCE)IR.1943-4774.0000052.

Vermote, E., Justice, C., Claverie, M., & Franch, B. (2016). Preliminary analysis of the performance of the Landsat 8/OLI land surface reflectance product. *Remote Sensing of Environment*, *185*, 46–56. http://dx.doi.org/10.1016/j.rse.2016.04.008

World Bank (2011). *Documento del Banco Mundial: Diagnóstico de la Gestión de los Recursos Hídricos en Chile.* Departamento de Medio Ambiente y Desarrollo Sostenible Región para América Latina y el Caribe. 78 pp, https://documents.worldbank.org/curated/en/452181468216298391/pdf/633920ESW0SPAN0le0GRH0final0DR0REV-0doc.pdf

Appendix A

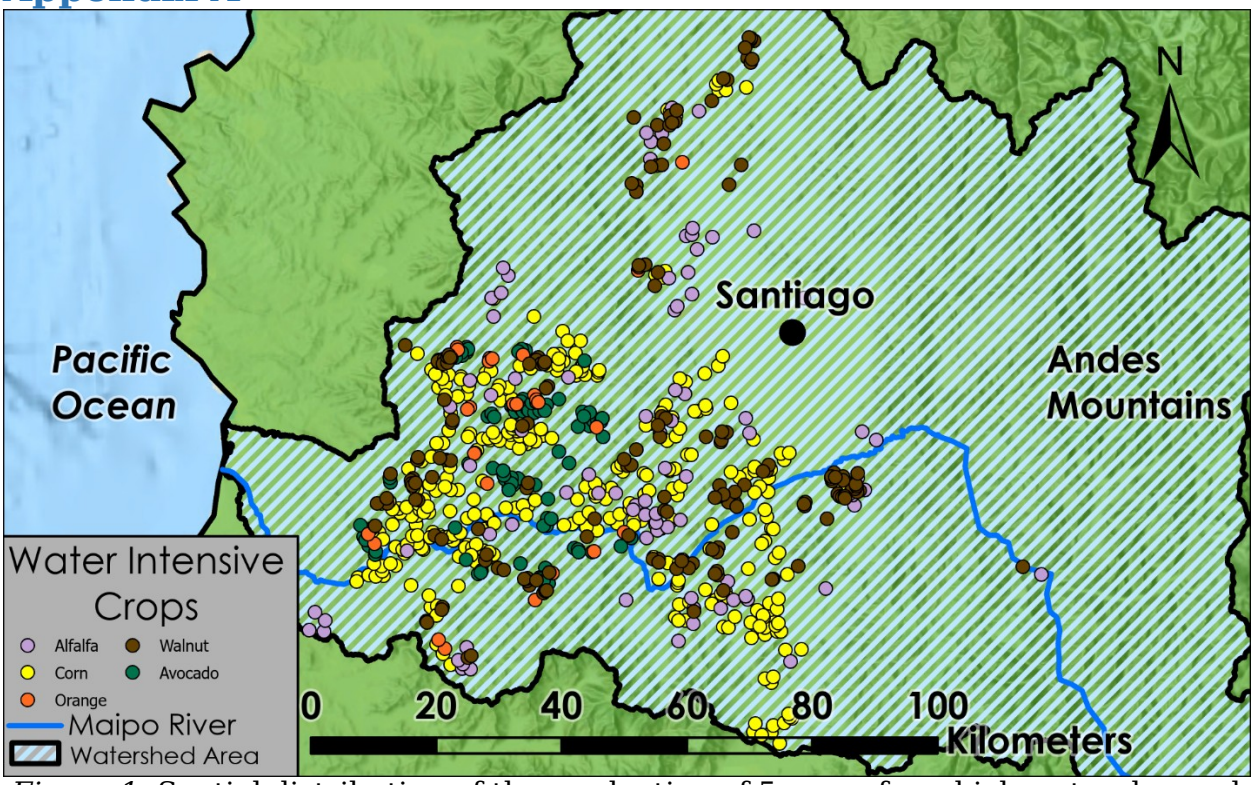

Figure 1. Spatial distribution of the production of 5 crops for which water demand was of concern to our partners. [Base map credits: Esri, USGS, CGIAR, WWF, CIREN, IDE Chile]

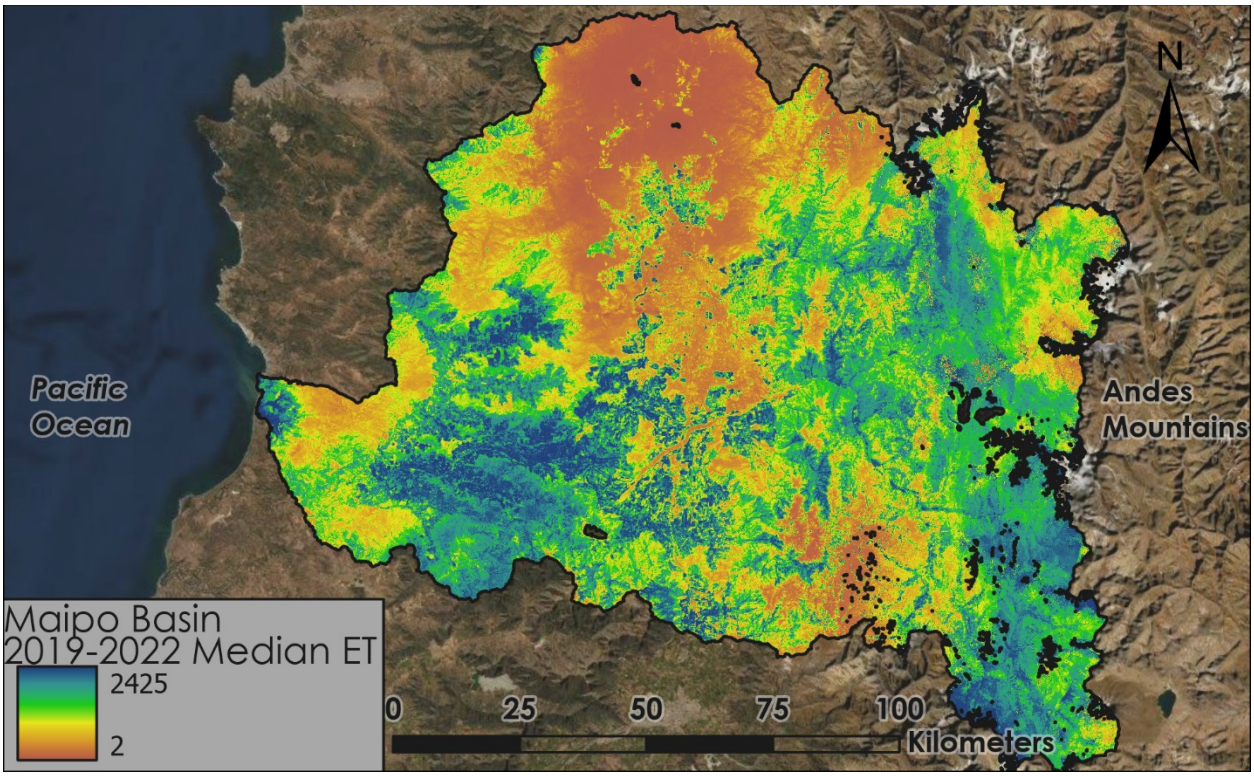

Figure A2. Spatial variability in the median of ECOSTRESS daily ET across the Maipo River basin from 2019 to 2022. [Base map credits: EarthStar Geographics, NASA, Esri, IDE Chile]

Appendix B

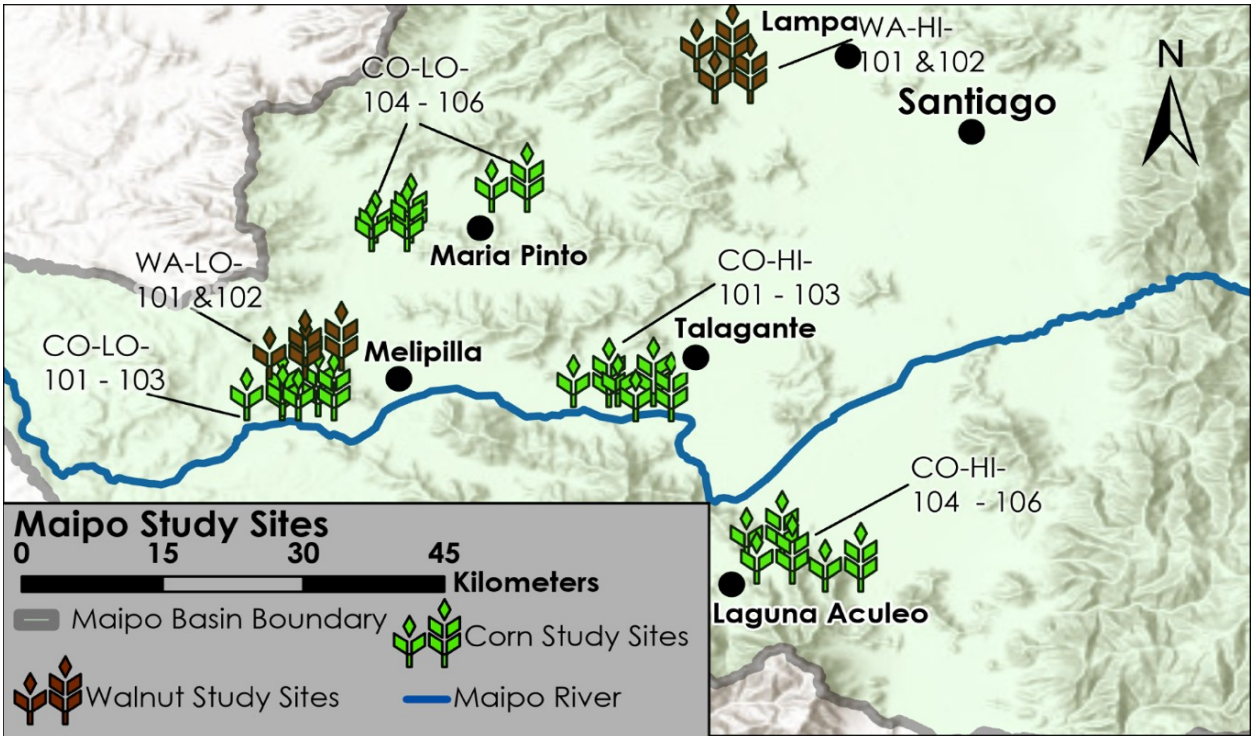

Figure B1. Location of study sites across the Maipo River basin in the vicinity of localities of particular interest to partners. [Base map credits: Esri, HERE, Garmin, Foursquare, FAO, METI/NASA, USGS, CGIAR, WWF, CIREN, IDE Chile]

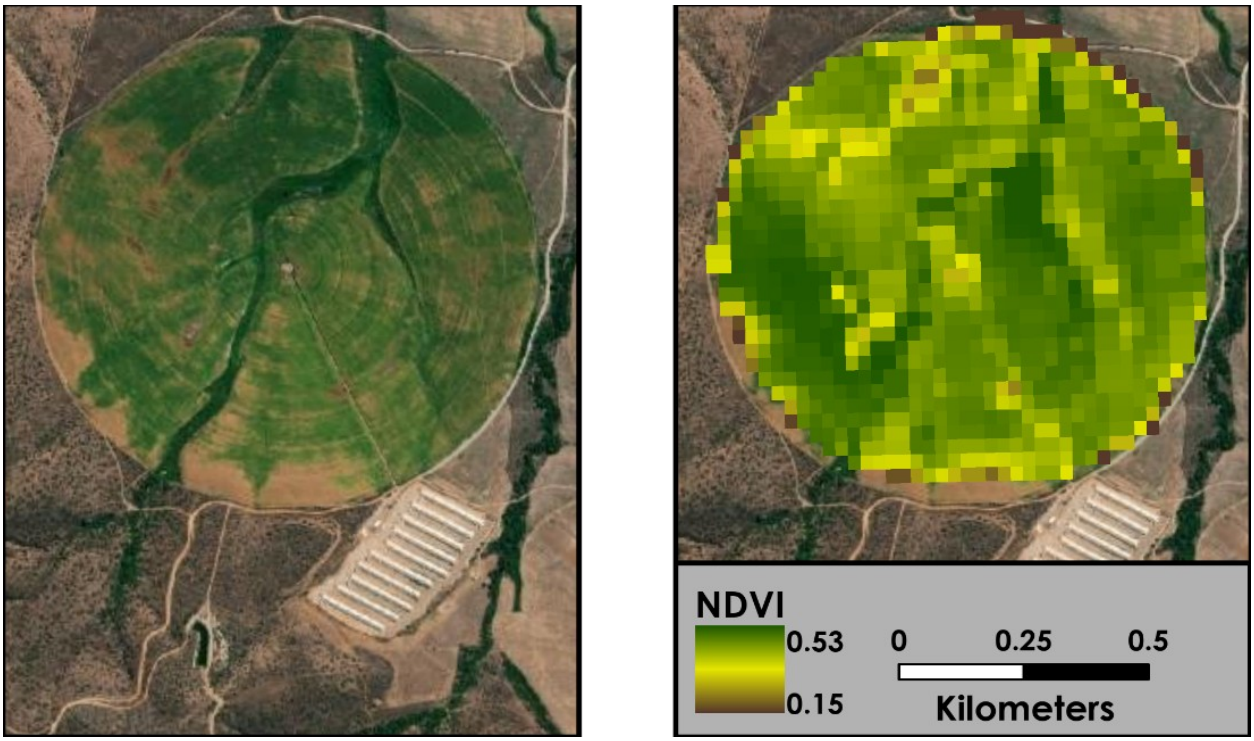

Figure B2. Daily snapshot of NDVI at irrigated maize field CO-LO-101. [Base map credits: Maxar, NASA, Esri]

Appendix C

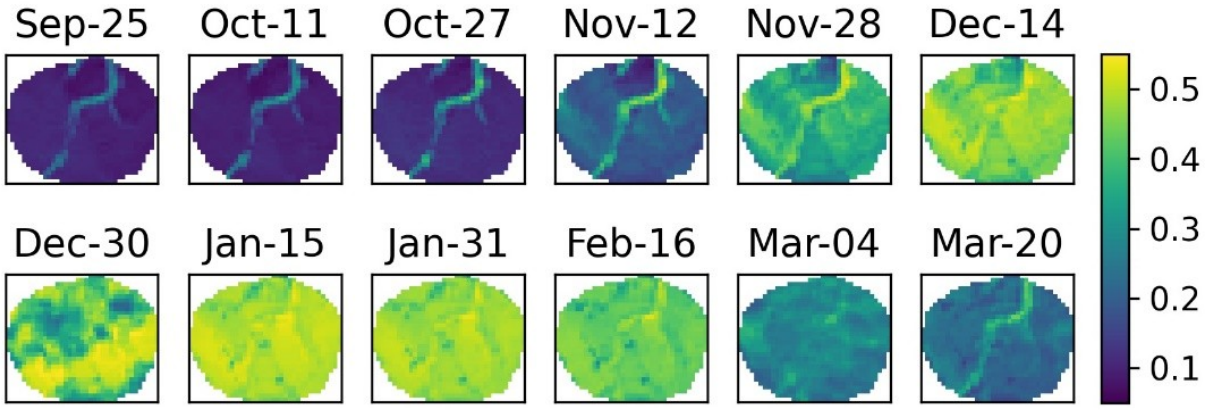

Fi*gure C1*. Spatial distribution of NDVI for site CO-LO-101 over the growing season 2021–2022. NDVI successfully captured the different growth stages of maize such as sowing, flowering and harvesting.

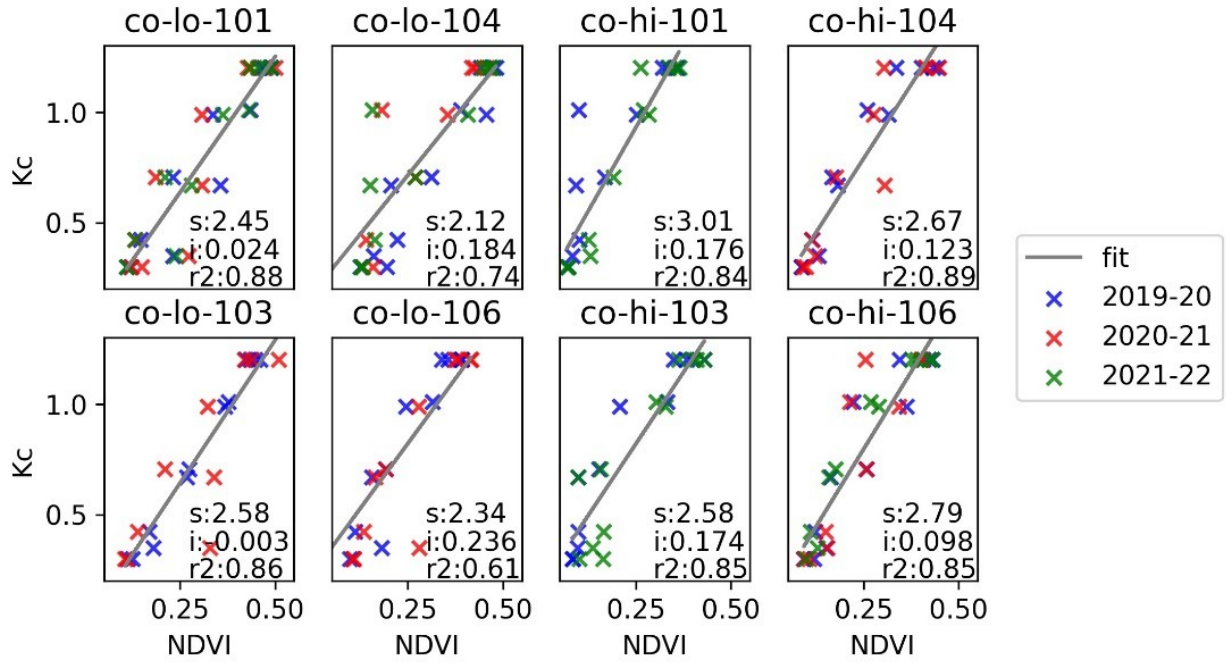

Figure C2. Linear Regression of Kc from FAO with respect to NDVI for 8 maize sites across 3 growing seasons.

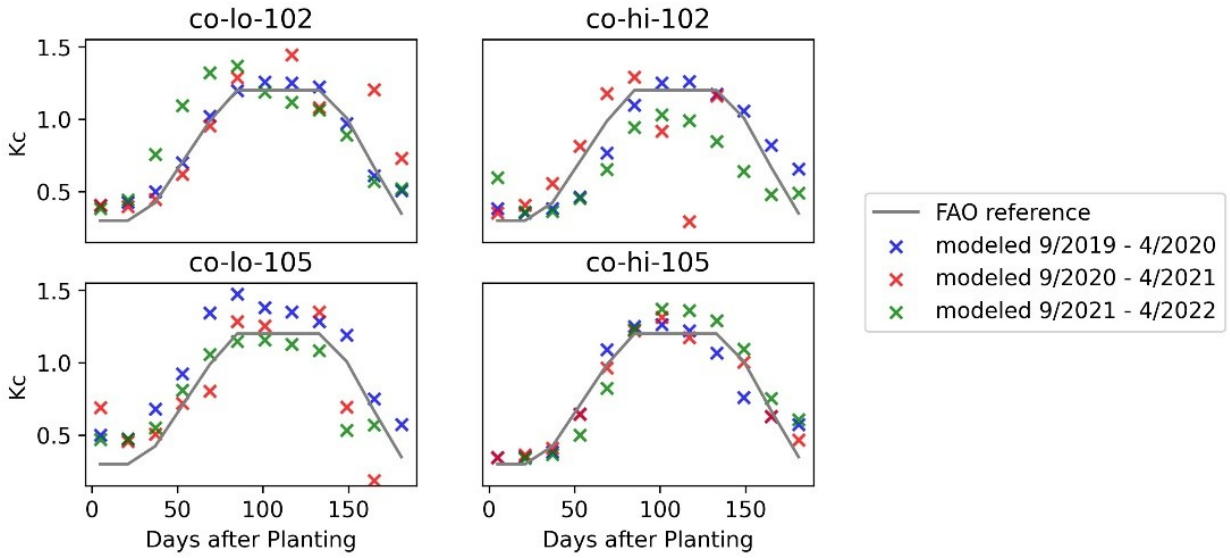

Figure C3. NDVI-Kc ensemble validation at 4 maize sites over 3 growing seasons. NDVI–Kc values for the 4 validation sites closely followed the FAO–Kc curve.

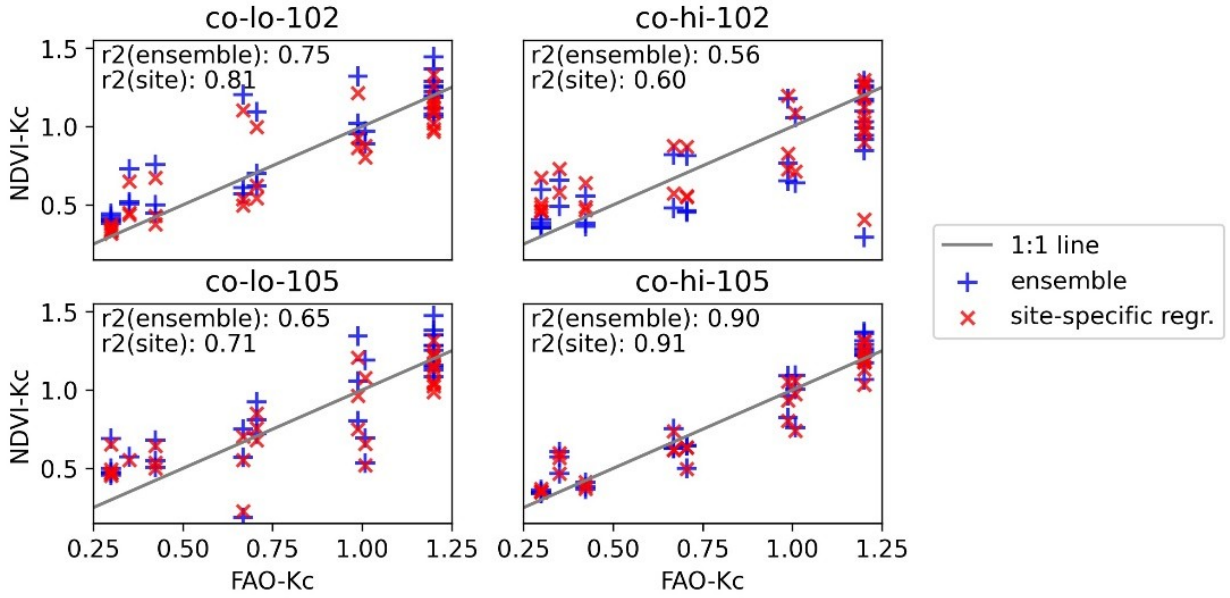

Figure C4 Performance of NDVI-Kc ensemble at maize validation sites over the 2019–2022 growing seasons.

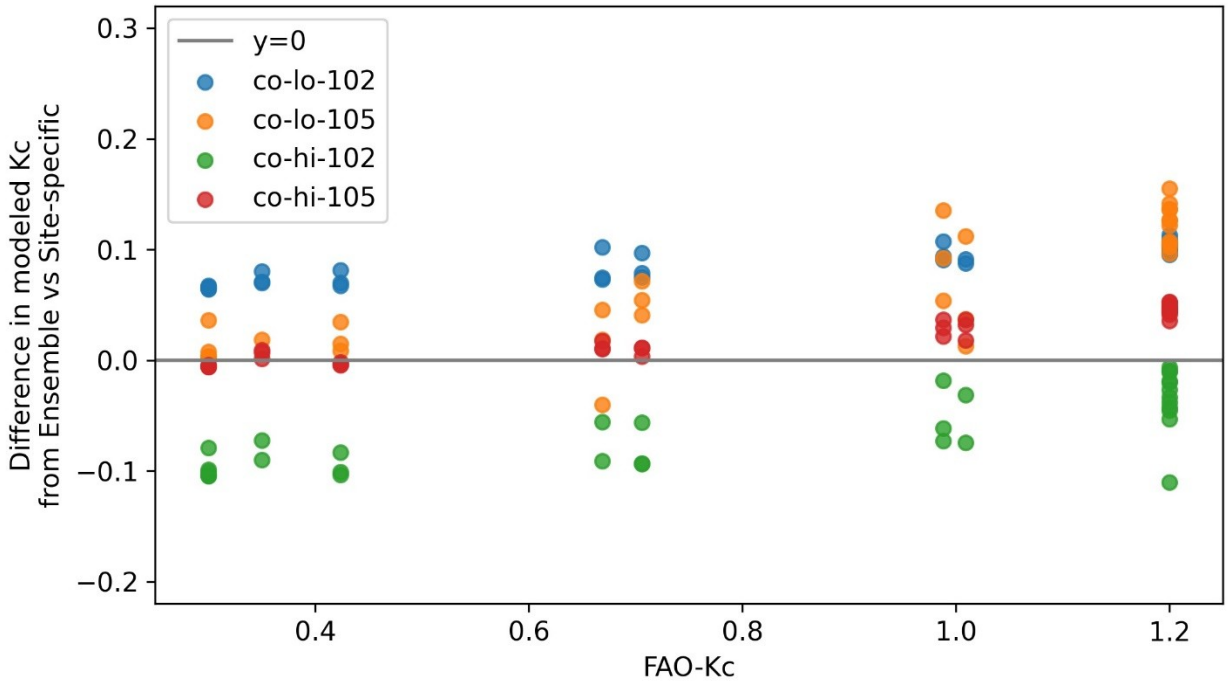

Figure C5. No particular bias of NDVI-Kc ensemble at maize validation sites over growing seasons 2019–2022.

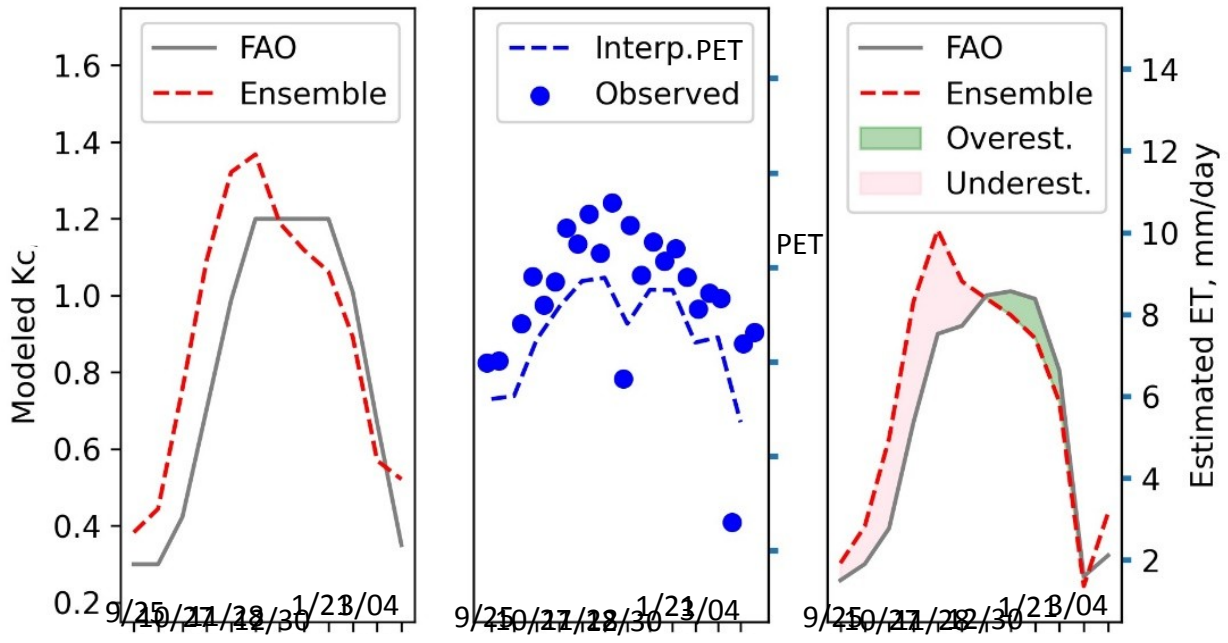

Figure C6. Applications of ensemble Kc model (left) along with PET (middle) for water requirement estimation (right) at maize site CO-LO-102 in growing season 2021–2022.

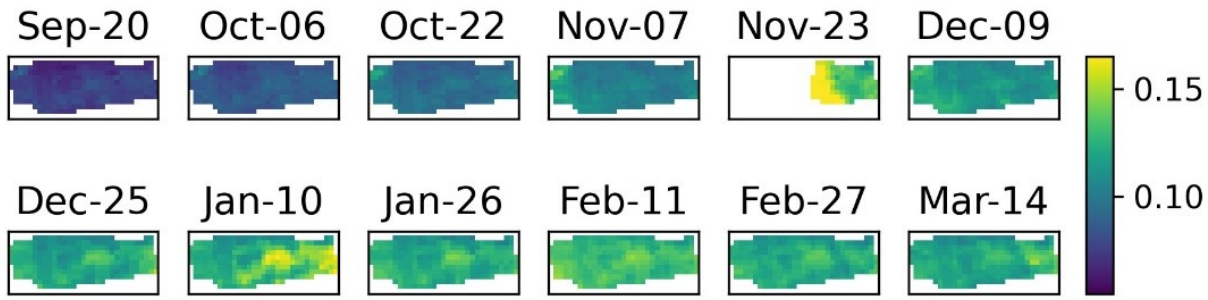

Figure C7. Spatial distribution of NDVI for field WA-LO-101 over the growing season 2019–2020. NDVI did not capture meaningful variations over the successive growth stages of the English walnut such as flowering, defoliation, and harvest.

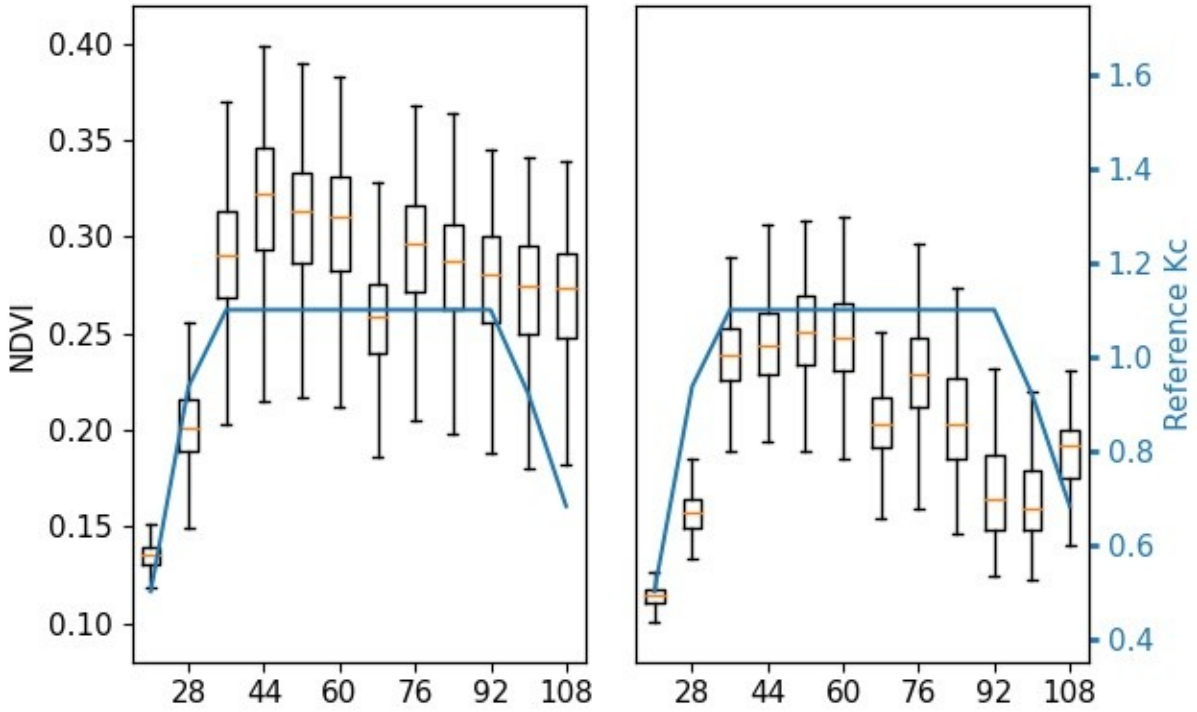

Figure C8. NDVI curve for sites WA-HI-101 and WA-HI-102 over the growing cycle 2019–2020. Duration of mid-season at either of the high sites appears to be longer (left) or shorter (right) than the reference Kc curve from FAO.

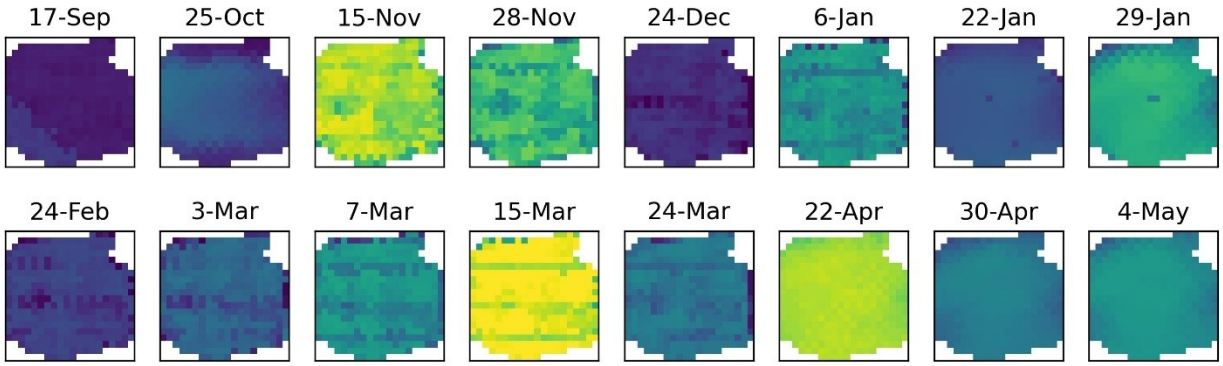

Figure C9. Spatial distribution of ECOSTRESS ET for site WA-LO-101 over the growing season 2021–2022. ET showed sharp variations across observations with no fixed revisit period over the season and time of day.

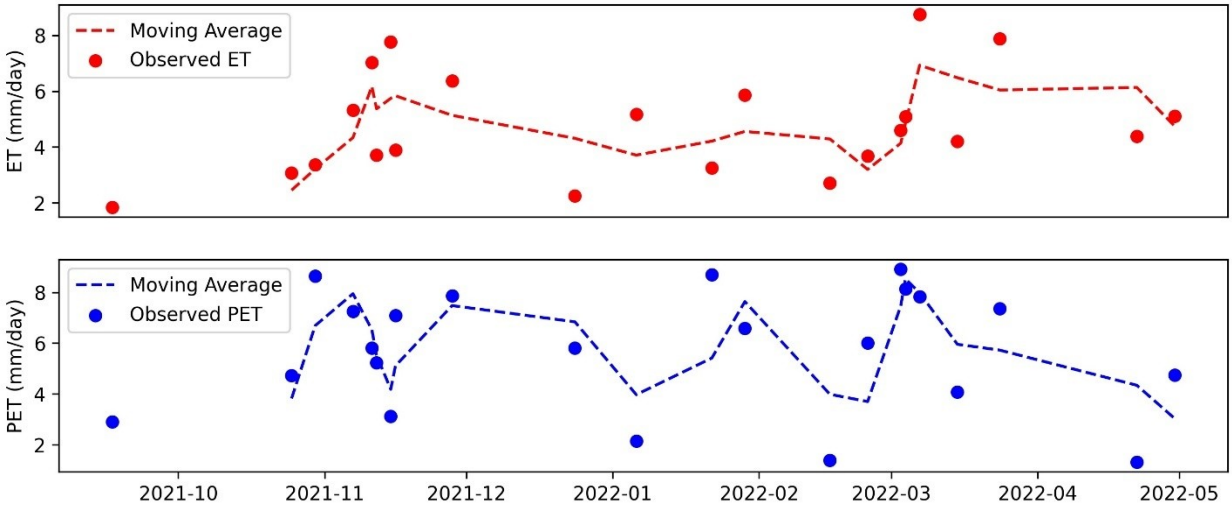

Figure C10. Trend and variability in ET and PET from ECOSTRESS at site WA-LO-101 in growing season 2021–2022.